Journal of Petroleum
Science and Technology

Analysis of the Photo Conversion of Asphaltenes Using Laser Desorption Ionization Mass Spectrometry: Fragmentation, Ring Fusion, and Fullerene Formation

Socrates Acevedo [1]*, Henry Labrador [2], Luis Puerta [2], Brice Bouyssiere [3] and Hervé Carrier [4]

[1]Universidad Central de Venezuela, Facultad de Ciencias, Escuela de Química, Caracas 1053, Venezuela
[2]Universidad de Carabobo, FACYT. Departamento de Química, Lab. Petróleo, Hidrocarburos y Derivados(PHD), Valencia Edo. Carabobo.
[3]CNRS / UNIV Pau & Pays de l'Adour, Institut des Sciences Analytiques et de Physico-Chimie pour l'Environnement et les Matériaux, LCABIE, UMR 5254, 64053 Pau, France.
[4]CNRS/TOTAL/UNIV PAU & PAYS ADOUR, LFCR-IPRA UMR 5150, 64000, PAU, FRANCE, Av. de Université-BP1155-64013. Pau, Cedex France.

ABSTRACT

The conversion or photo conversion of asphaltenes to polycyclic aromatic hydrocarbons (PAH's) promoted by a laser source is analyzed using both experimental and theoretical methods. We propose that during measurements performed at an intermediate laser power, fragmentation to afford PAH's and ring fusion to yield fused PAH's (FPAH's) may occur either within molecular clusters (resin case) or within molecular aggregates (asphaltene case) which are vaporized or sublimed after ionization by the laser source. These events change the initial molecular mass distribution (MMD) of the sample to a continuous statistical MMD that can be fitted to a log-normal distribution. At a high laser power, the experimental MMD is converted to a sequence of C_n bands (n is an even number) which are separated by a 24-amu, the characteristic of a mixture of fullerene compounds.

Keywords: LDI, Asphaltenes, Photo Conversion, PAH's, Fullerenes

INTRODUCTION

The formation of photocompounds during laser desorption ionization mass spectrometry (LDI MS) examination of asphaltenes and other carbonaceous materials is becoming an important research area related to fullerene and carbon nanotube formation, extra-terrestrial bodies, and, of course, asphaltenes. Several research groups have presented spectra showing a 24-amu difference, corresponding to C_2. These spectra are produced when asphaltene or other carbonaceous materials are examined by LDI MS.

When asphaltenes were examined using LDI (+)-FT-ICR MS, asphaltenes showed a wide Gaussian band extended from 500 to 2000 Da with a 24-Da separation over the entire range. These bands, promoted by laser power, were attributed to fullerene-type materials [1] Similar results were reported by Rizzi et al. in 2006 [2] when Italian asphaltenes were analyzed using LDI and SALDI MS techniques. The abovementioned sequential band of 24 Da, which was found in a wide band

***Corresponding author**
Socrates Acevedo
Email: socrates.acevedo@gmail.com
Tel: +58 41 2048 4818
Fax:+58 41 2048 4818

Article history
Received: December 15, 2016
Received in revised form: April 11, 2017
Accepted: May 10, 2017
Available online: May 22, 2018
DOI: 10.22078/jpst.2017.2385.1414

extending from 500 to 2000 Da and beyond, was promoted by the laser and attributed to the formation of polycyclic aromatic hydrocarbons (PAH's) [2]. Carbon clusters or fullerenes with a typical 24-amu separation were reported for a vacuum residue examined using LDI [3]. The examination of PAH's under LDI MS conditions similar to the one employed for asphaltenes led to the formation of multimers of these PAH's [4]. Authors have ascribed these multimers to the presence of non-covalent clusters during the desorption process [4]. Apicella and co-workers have also reported both multimer formation and fragmentation when PAH's were studied using LDI. The abovementioned 24-amu sequence was also observed when a soot sample was studied using LDI techniques [5]. Covalent clusters of PAH's were detected when they were examined using an LDI assisted by collision-cooling with nitrogen as the inert gas [6]. According to these authors [6], the collisions of radical ions with the gas molecules dissipate energy, thereby reducing unwanted reactions such as fragmentation. However, C-H and C-C fragmentations were observed as there were covalent clusters with a molecular mass of 2M-4H, in which M is the mass of the parent cation radical and the dimer lost 4 hydrogens during the fusion of two PAH's [6,7] . A statistical MMD comprising a sequence of bands separated by 24 amu was reported by Santos et al. after the examination of an asphaltene sample using LDI MS [8]. When a mixture of polycyclic aromatic hydrocarbon standards was examined under similar conditions, it afforded a similar MMD that allowed the authors to conclude that these MMD were the result of PAH fusion and the formation of fullerene-type homologous photocompounds. According to these authors [8], the "C_2 sequence" has been observed previously [9,10], and was erroneously ascribed to the compounds present in the sample under analysis. The C_2 sequence was also found during the LDI treatment of Hassi-Messaoud asphaltenes [11] and Algerian asphaltenes [12]. Becker et al. in 2008 [13] used LDI MS combined with ion mobility to study asphaltenes and DAO, and observed fullerenes only in the case of asphaltenes. High resolution transmission electron microscopy (RTEM) was used for the detection of fullerenic structures in crude oils [14]. Traveling wave ion mobility (TWIM) was combined with LDI to separate fullerenes from other asphaltene components formed during LDI MS experiments. The technique employed gives a two-dimensional plot where fullerenes are clearly distinguished from other components [15].

Mass spectra showing the removal of hydrogen from cation radicals to afford multiradicals (diradicals, triradicals, and so on) under the energy environment provided by a laser (henceforth, laser conditions) were reported in 2014 [16]. Thus, all the hydrogens of the PAH cation radical $[C_{66}H_{26}]^+$ were removed as laser power steadily increased. MMD obtained using SEC with a UV detector leads to a log-normal distribution when octylated asphaltenes (OA) are used as the sample [17]. Presumably, the octyl groups inhibit the column-sample interaction responsible for the long tail and band deformation typical of the SEC of asphaltenes. Due to the employment of a UV detector, the observed MMD corresponds to the random distribution of PAH's comprising the core of the asphaltene molecules.

The reported LDI mass spectra of asphaltenes and octylated asphaltenes with up to five octyl groups

per 100 carbons showed a similar MMD, indicating that these alkyl groups have no impact on the MMD obtained. As is now recognized [8], the obtained MMD corresponds to a log-normal distribution of fused PAH's (see below). A combination of LDI, SALDI, and L^2MS techniques led authors to propose the presence of asphaltene nanoaggregates in the vapor phase [18], and, according to other authors, the use of ion mobility techniques confirm aggregate formation in the gas phase for molecules with an MM > 3000 Da [13]. The partial fragmentation of alkylated PAH was observed during its analysis with desorption/ionization two laser μL^2-MS equipment [19], a technique employed to reduce or suppress fragmentation and ring fusion. When LDI MS was employed to measure the MMD of asphaltenes obtained after evaporation from toluene solutions, a large shift to a higher MM was observed. The authors ascribed this finding to asphaltene aggregates presented in the sample [20]. LDI MS applied to Algerian [11] and asphaltenes from another source [21] also confirmed the C_2 sequence referred to above. Curved PAH structures, containing five member rings such as corannulene and corannulene derivatives, were proposed by Pope et al. as the precursors of fullerene structures [22,23].

EXPERIMENTAL PROCEDURES

Materials and Methods

Asphaltenes and resins, both from Venezuela, were obtained by routine methods described elsewhere [24]. Briefly, corresponding crude oils mixed with toluene (1:1) were diluted (at a ratio of 1:60) with heptane, and the flocculated asphaltenes were filtered and dried. The resins were obtained after the extraction of asphaltenes in a Soxhlet using boiling n-heptane. Asphaltenes were obtained from Cerro Negro (CN) and Furrial crude oils, while the resins were obtained from Furrial crude oil.

Equipment

LDI MS TOF was determined using a laser desorption ionization system with a time-of-flight mass spectrometer (LDI TOF MS Voyager DE-STR Applied Biosystems Instrument). The laser system comprised a 337 nm-N_2 excimer laser at 20 Hz, which was used to analyze diluted (approximately 100 $mg.L^{-1}$) tetrahydrofuran solutions. These solutions were spread on the sample holder, and after solvent evaporation, these solutions were introduced into the LDI system under vacuum. The TOF detector was used in the linear mode, and the laser shots (LS) or laser powers were in a range of 1500 to 3000. No signal was detected below the LS equal to 1500.

Methods

The semi-empirical quantum mechanical method PM6, developed by Stewart et al. in 2007, was used for the required calculations [25].

The ionization and fragmentation of asphaltenes leading to the formation of PAH systems, along with ring fusion to form larger systems (FPAH's) and C_2 sequence fullerene are the processes considered herein. The route examined here is shown in the scheme below (Figure 1); all the stages are promoted by the laser source, where the power increases from one stage to the next in an LS range of 1500 to 3000.

In the first stage, asphaltene aggregates are ionized to a cation radical (CR) and sublimed from a condensed state that could be either the solid state or the plume.

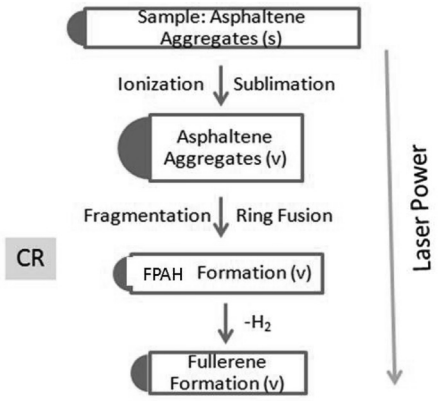

Figure 1: A schematic representation of the sequence of events promoted after laser contact with the sample. Ionization to a cation radicals (CR) and sublimation occurs in the first stage followed by fragmentation and ring fusion to afford FPAH ion radicals at a higher laser power. At even a higher laser power, the dehydrogenation of FPAH's is followed by fullerene formation. The letters "s" and "v" stand for solid and vapor respectively.

Once in the vapor phase as aggregates, the sample undergoes the fragmentation and ring fusion to afford FPAH's in the second stage. Finally, after H_2 is lost, fullerenes are formed in the third stage. Relevant fragmentation, multiradical formation, and the formation of FPHA's and fullerene-type materials were simulated and calculated with convenient models using PM6. In this work, multiradicals are defined as the structure resulting after the removal of all or some hydrogen from the corresponding PAH.

For the resin samples, the scheme is similar to the one presented in Figure 1 with the following differences; after ionization to a CR, a molecular cluster is evaporated. After fragmentation and fusion, the cluster is converted to FPAH's. No fullerene formation was observed in this case within the same LS range used for asphaltenes.

Thermodynamic Parameters

Thermodynamic parameters were calculated at different temperatures using the PM6 method. Molar entropies were obtained at the required temperature from the frequency facility of the PM6 method. The calculation is illustrated by the reaction scheme given below:

$$A + B \xrightarrow{hv} C + 2H_2 \quad (1)$$

where, *A* is a CR, and *B* is a neutral reactant; *C* comes from the fusion of *A* and *B*. In this photoreaction, two moles of hydrogen are produced when two moles of reactant are consumed. For each component, the geometry was optimized, and the entropy *S* was calculated at the required temperature (*T*). The following changes were then computed:

$$\Delta S_R = \frac{2S_H + S_C - S_A - S_B}{2} \quad (2)$$

$$\Delta S_{PAH} = \frac{S_C - S_A - S_B}{2} \quad (3)$$

where, ΔS_R is the overall entropy change, and ΔS_{PAH} is the entropy change of the PAH species. These changes were evaluated in a temperature range of 500 to 1000 K.

For these calculations, the reaction between one pyrene molecule and its CR homolog was used to afford a dimer CR of a molecular mass of 2M-4, where M is the molecular mass of pyrene. This occurs according to the reaction given below (Figure 2):

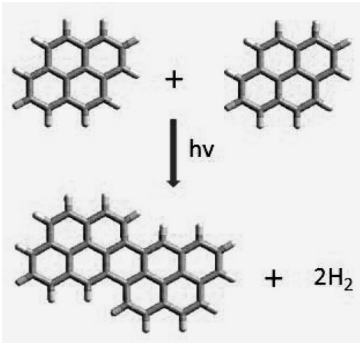

Figure 2: The reaction between one pyrene molecule and its CR homolog.
It should be noted that the MM of pyrene dimer is 2M-4. This dimer was detected when pyrene was examined with LDI MS under the conditions of collision cooling [16].

Closed or Fullerene-type Structures

The few fullerene-type and curved surface structures considered herein were constructed using the isolated pentane rule (IPR), in which no two pentagons share an edge [8]. When required, these structures were calculated using the PM6 method.

The number-(M_n) and weight-(M_w) average molecular masses were obtained using Equations 4 and 5.

$$M_n = \frac{\sum_i n_i M_i}{\sum_i n_i} = \frac{\sum_i I_i M_i}{\sum_i I_i} \quad (4)$$

$$M_w = \frac{\sum_i n_i M_i^2}{\sum_i n_i M_i} = \frac{\sum_i I_i M_i^2}{\sum_i I_i M_i} \quad (5)$$

The geometric mean (M_g) of these values was obtained using Equation 6.

$$M_g = \sqrt{M_n M_w} \quad (6)$$

where, n_i, I_i and M_i are the corresponding number of molecules, intensity, and molecular mass respectively. The intensity and molecular mass were determined from the experimental results.

Log Normal MMD

For statistical MMD, the log-normal distribution was used, which is easily obtained as follows:

The error distribution could be defined using Equation 7:

$$dP = \frac{1}{\sigma'\sqrt{2\pi}} \exp\left[-\frac{1}{2}\frac{(x-x_0)^2}{\sigma'^2}\right] dx \quad (7)$$

As usual, *dP* is the probability of finding the value of *x* between *x* and *x+dx*. Herein, x_0 is the mean, and σ' is the standard deviation. Now, the variable can be changed in a way that $x = \log M$, which leads to Equations 8 and 9.

$$dP = \frac{1}{\sigma\sqrt{2\pi}} \exp\left[-\frac{1}{2}\frac{(\log M - \log M_0)^2}{\sigma^2}\right] d\log M \quad (8)$$

$$dP = \frac{1}{M\sigma\sqrt{2\pi}} \exp\left[-\frac{1}{2}\frac{(\log M - \log M_0)^2}{\sigma^2}\right] dM \quad (9)$$

where σ, *M*, and M_0 are the standard deviation, the molecular mass, and the molecular mass mean. Equation 10 was used for fitting.

$$y = y_0 + \frac{A}{M\sigma\sqrt{2\pi}} \exp\left[-\frac{1}{2}\frac{(\log M - \log M_0)^2}{\sigma^2}\right] \quad (10)$$

RESULTS AND DISCUSSION

Fragmentation and Ring Fusion

Figures 3 and 4 show a series of LDI MS spectra taken of Furrial and CN asphaltene samples at different laser powers (LS's).

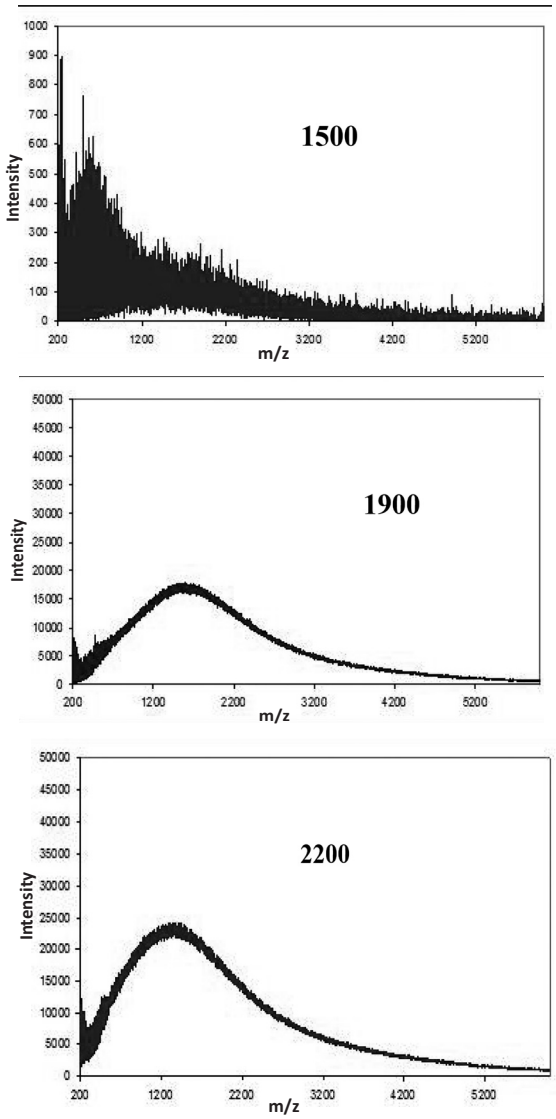

Figure 3: Sequences of LDIMS of asphaltenes (Furrial) measured at increasing LS power. The increase in LS apparently promotes both fragmentation and ring fusion, as suggested by the observed large MMD changes observed in this LS range (200-5200 amu range).

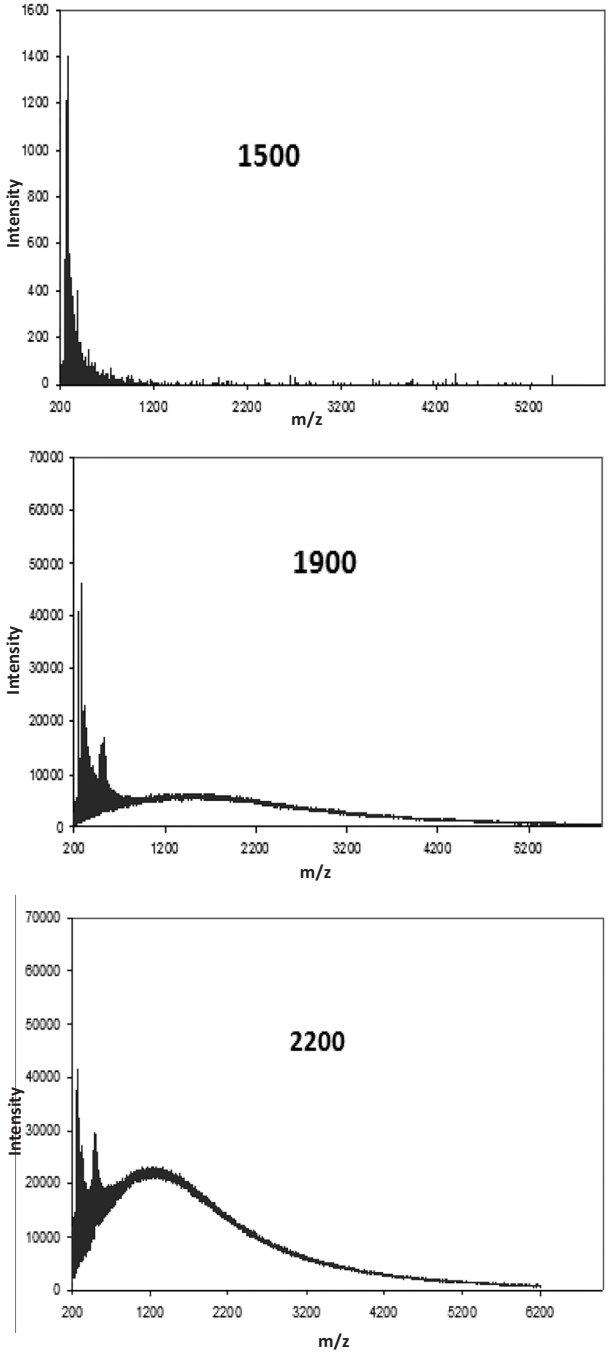

Figure 4: Sequences of LDIMS of CN asphaltenes measured at increasing LS power. Evidence for ring fusion is apparent from LS = 1900 onward in this LS range(200-5200 amu).

Apparent conversion to FPAH's was also observed for the resins (Figure 5).

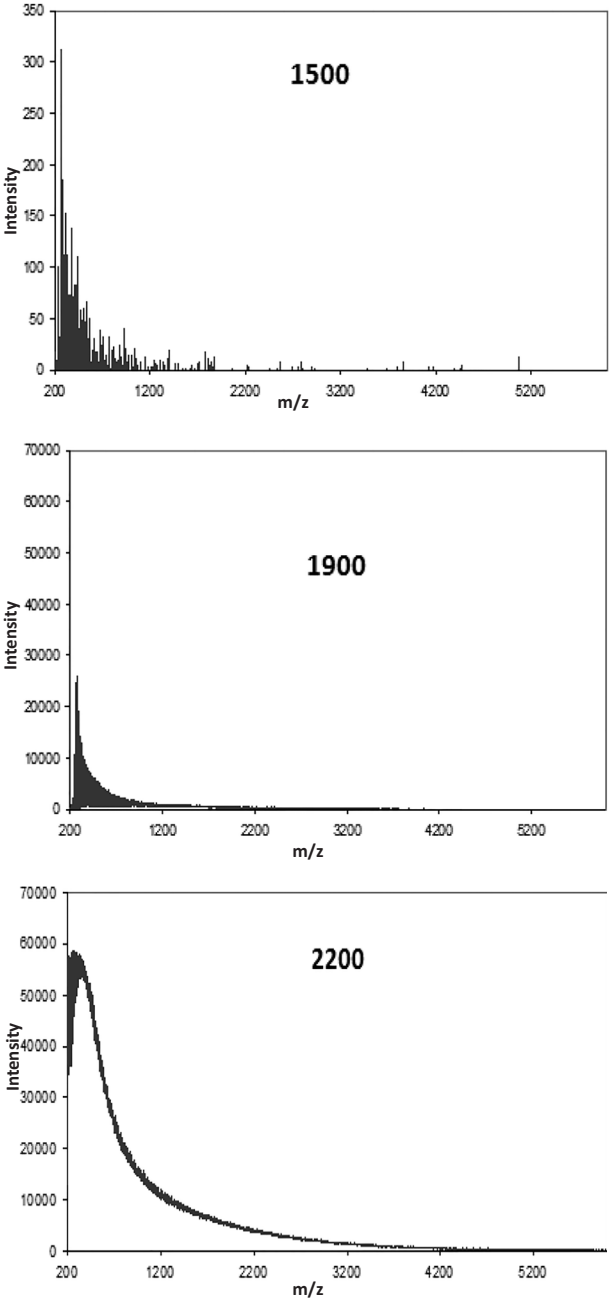

Figure 5: Resin spectra measured at different relative laser powers (LSs) in the range of 200 to 6200 m/z. Apparently, as LS increases, the sample is steadily converted to a mixture of FPAH's.

The sequence shows how the initial sample changes when the LS increases to the point where fragmentation is readily apparent as the initial complex distribution is converted to a quasi-continuous MMD. This result is coherent with the simultaneous operation of both fragmentation and

ring fusion and with the mass maxima shown by these samples in Figures 6 and 7.

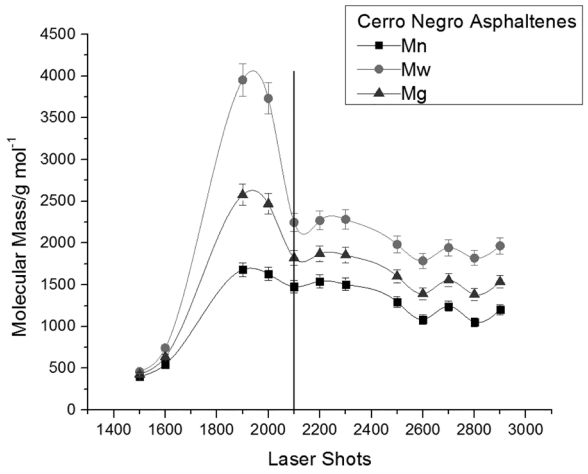

Figure 6: Dependence of molecular mass on LS for CN asphaltenes. The maximum below LS = 2100 is consistent with the simultaneous operation of ring fusion and fragmentation, which have opposite effects on the sample mass. The sector to the right of LS = 2100 corresponds to fullerene formation and the loss of hydrogen and other elements such as nitrogen, sulfur, and oxygen.

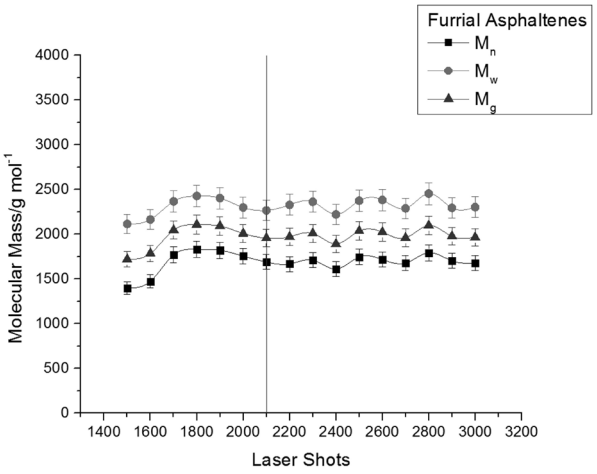

Figure 7: Dependence of the molecular mass on LS for Furrial asphaltenes. The maximum below LS = 2100 is consistent with the simultaneous operation of ring fusion and fragmentation, which have opposite effects on the sample mass. The sector to the right of LS = 2100 corresponds to fullerene formation and the loss of hydrogen and other elements.

The increase in the mass of ring fusion is opposed by fragmentation (mass decrease). As described above (see Introduction), fragmentation and ring fusion have been observed using model PAH's [4,6,19]. At an LS value larger than about 2100, a series of maxima and minima are observed; however, it appears that most of these values are within the experimental error suggesting that sample has been converted to stable derivatives such as fullerenes.

It is likely that in this case, the sample is vaporized as molecular clusters, thereby promoting ring fusion. The molecular mass distribution of PAH coming from ring fusion (MMDRF) could be well fitted to a log-normal statistical distribution, as shown in Figure 7.

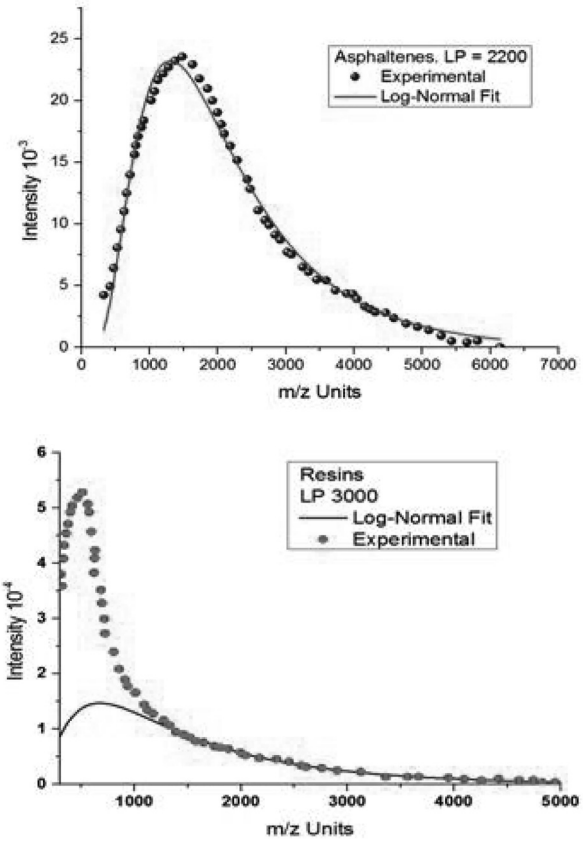

Figure 8: Fitting a log-normal distribution (Equation 10) to experimental data for the asphaltenes (top) and the resins (bottom) at the shown laser power. Apparent conversion to FPAH's is complete for the asphaltenes and partial (approximately 60%) in the case of the resins.

Log-normal distribution was well fitted to the experimental data only at the tail of the mass spectra of the resins; for asphaltenes, conversion to ring fusion was complete, whereas for the resins it was approximately 60%. The parameters corresponding to these fits are collected in Table 1.

Table 1: Log-normal fitting parameters.

Sample	M_0	σ	y_0	A	Adjusted R^2
Asphaltenes	1863	0.596	-151.2	5.47E+07	0.98
Resins	676	0.8	-289	3.00E+04	0.99

See Equation 10 for parameter definition.

In comparison with the asphaltenes, the resins have higher and faster volatility, which could account for their partial conversion; they are also consistent with the higher LS value required for ring fusion.

Previously, MMD's obtained from LDI-MS were also fitted by a log-normal distribution [4,27].

Asphaltene molecules are thought of as aromatic cores with a high substitution of hydrogen in the form of aliphatic chains [28]; in other words, they contain a very low percentage (approximately 5%) of aromatic hydrogens [24]. This means that for sufficient laser power (see Figures 2 and 3), the fragmentation of alkyl chains would result in the formation of very reactive multiradicals, which, if close enough, will react with the nearest neighbor homologs, leading to ring fusion and to a random MMD.

Figure 7 is a simple depiction of fragmentation using molecular models. Because multiradicals are extremely reactive, they could react to form new 6- or 5-member aromatic rings.

The presence of diradicals is possible only in the presence of the high energy provided by the laser. Fragmentation could occur either by direct energy coming from the laser or by contact with highly excited CR or homologs (see Figure 9 for an example of this process).

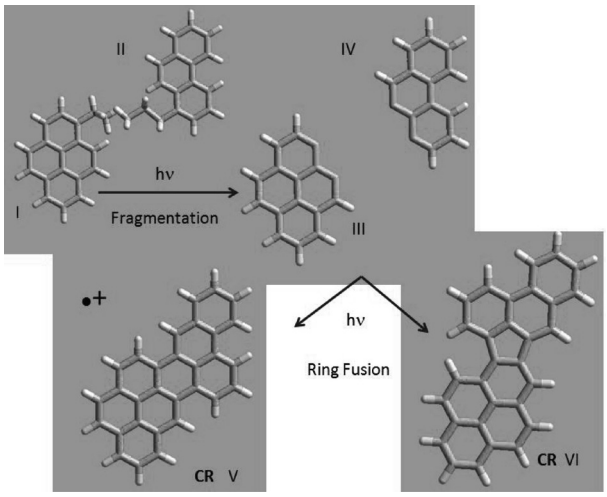

Figure 9: An example of ring fusion considered herein, in which the alkyl aromatics, represented by 1-ethyl-pyrene (I) and 4-ethyl-anthracene (II), are fragmented by the laser to afford diradicals III and IV, which leads to fused system V or VI cation radicals (CR).

Ring fusion in the open vapor phase is unlikely to occur. The gathering of many molecules in the vapor state would have a high entropic cost, as suggested by the calculations shown in Table 2.

Table 2: Entropy changes computed for the fusion of pyrene and the pyrene cation radical[a].

T/K	$T\Delta S$ /kCal.mol^{-1}	
	ΔS_R [b]	ΔS_{PAH} [c]
500	3.8	-26.0
600	4.9	-32.0
700	6.1	-38.2
800	7.1	-44.7
900	8.2	-51.4
1000	9.2	-58.4

The PM6 method; b: overall change; c: change between PAH species.

Although the overall $T\Delta S_R$ is positive, due to the formation of hydrogen, bringing the reactants together for the reaction to occur involves a large negative change in $T\Delta S_{PAH}$, which could severely impair or prevent all contacts among reactants. As shown in Table 2, this hindering effect increases with temperature.

Thus, photoreactions in the vapor phase are unlikely and expected to have a small or insignificant contribution to ring fusion and other possible photoreactions. For the fusion of three or more PAH's, larger, more negative $T\Delta S_{PAH}$ are obtained. Moreover, very high temperatures, in the range of 4000-8000 K, are expected in ns pulsed laser plasma commonly used in LDI [23].

On the other hand, due to close contact within an aggregate or cluster that has been evaporated or sublimed from the corresponding condensed state, ring fusion will more be favored for an associated mixture such as the asphaltenes. Of course, in this case, little contribution of ΔS_{PAH} to the reaction is expected. These arguments are congruent with the method employed in the L^2 MS technique described above, in which, to avoid ring fusion, the two lasers are tuned so that the first sublimes the sample and the second (the one used to ionize the sample) is shot at the vaporized sample a few μs later [19,27].

In view of the above comments and results, it is concluded that under the present conditions and after ion radical formation, the samples are either sublimed (the asphaltenes) or vaporized (the resins) as aggregates or molecular clusters respectively. Subsequently, they undergo fragmentation and ring fusion before being converted to fullerenes at higher LS values. As mentioned in Introduction, the presence of asphaltene nanoaggregates has been suggested in the vapor phase using a combination of LD techniques [4,18].

Fullerene Formation

Figure 10 shows the LDI MS spectrum of Furrial asphaltenes measured at an LS value of 2900.

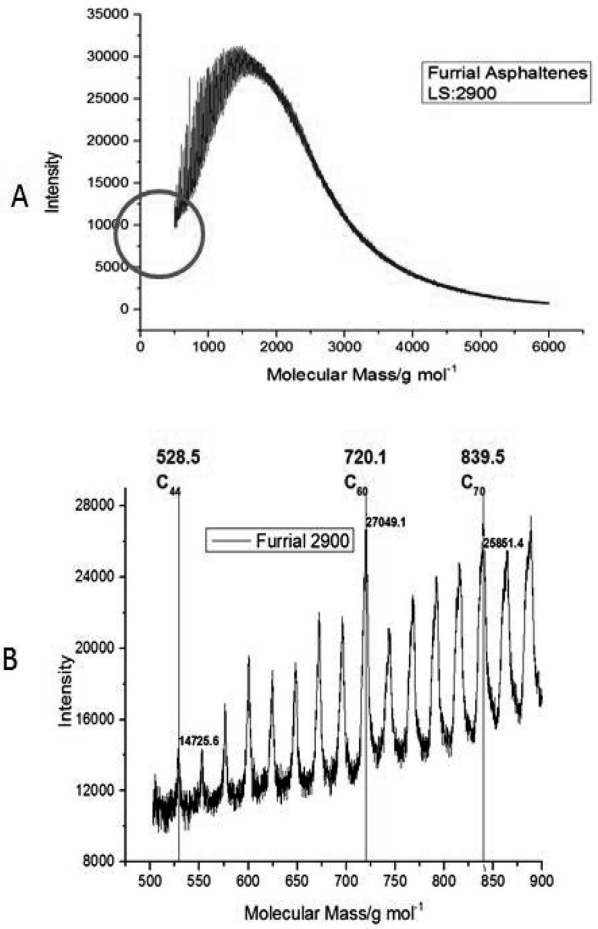

Figure 10: LDI spectra of Furrial asphaltenes measured at LS = 2900 laser power. A) full range; B: expansion of the 500-900 amu, corresponding to the inset range showing the C_2 = 12 amu band sequence. No fullerene bands were detected below 500 g mol^{-1} or above 2300 g mol^{-1}. Bands and intensities corresponding to C_{44}, C_{60}, and C_{70} are distinguished by vertical lines.

At this high energy, the sequence of C_2 bands shown in the expansion is very clear. We could detect fullerenes from C_{42} (MM = 720) to approximately C_{214} (MM = 2570). As suggested elsewhere [30,31], C_{60} and C_{70} are relatively stable fullerenes, and

this is consistent with the intensities of the corresponding bands (Figure 9-B). Similar results were obtained for CN asphaltenes (not shown). Thus, in view of similar findings regarding the C_2 sequence described in Introduction, this behavior appears to be a characteristic of asphaltenes under high laser energy conditions.

At energies high enough to promote the removal of hydrogens from C-H corresponding to the formed FPAH cation, multiradicals will form. These multiradicals are very reactive species; a hint of this is shown in Figure 11, where a very large and negative change in the enthalpy of formation could be estimated.

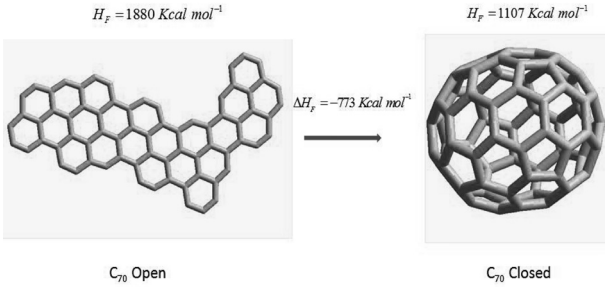

Figure 11: Depiction of the conversion of a multiradical cation C_{70} to a closed C_{70} cation radical fullerene type structure

As it is well known [22,23,30], the PAH's avoid the formation of multiradicals by forming curved surfaces in which the rupture of C-H would occur simultaneously with C_2 additions and C-C bond formation. These curved surfaces are formed after intramolecular rearrangements of the planar hexagonal structures of FPAH's, which become curved after the inclusion of pentane rings.

A plausible evolution of some stages leading to C_{72} is shown in Figure 12.

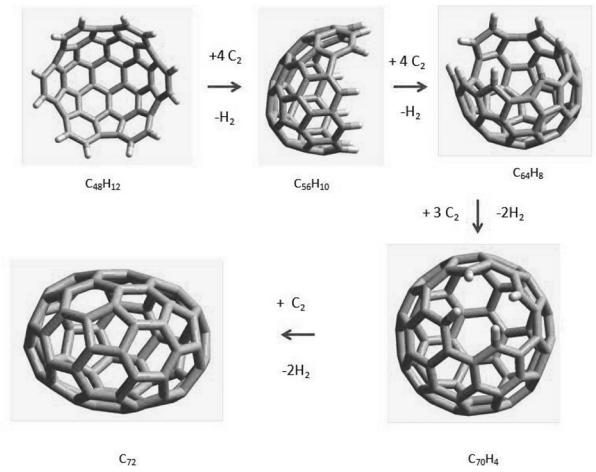

Figure 12: A schematic representation of the formation of the fullerene-type structure C_{72} by means of progressive stages in which the growth of the spheroid surface, after C_2 transfer, allows for hydrogen loss without the formation of multiradicals. Transfer of C_2 is intramolecular and comes from somewhere else within the molecule (not specified for simplicity).

It should be mentioned that, by using appropriate computation algorithms, it is possible to build fullerenes to the required size and molecular mass [32]. In this way, the observed C_2 sequence can be possible in terms of the above arguments irrespective of the fullerene size.

It should also be mentioned that heteroatoms initially present in the asphaltene sample should be removed at some stage during laser contact; otherwise, the observed C_2 band sequence will not exist. It is also interesting that under the same LS used for the asphaltenes, the resins do not yield fullerenes. Finally, it is very important to remark that, as it is the case for fullerenes, the statistical molecular mass distribution obtained at low and medium values of laser power for the asphaltenes is an artifact produced by laser contact with the sample and is not at all the proper molecular mass distribution of the asphaltenes. Thus, some previous results regarding this issue need revising [27].

CONCLUSIONS

The sublimation of aggregates (the asphaltenes) and the vaporization of clusters (the resins) were found out to be consistent with both fragmentation and ring fusion. The fragmentation promoted either by the laser or by contact with high energy homologs leads to very reactive PAH multiradicals, which, in contact with each other in the aggregates or clusters, result in ring fusion and in the formation of FPAH's having a log-normal MMD. At a high laser power, hydrogen is removed from FPAH's, leading to a typical fullerene MMD in which each band is separated from the next by C_2 amu. It could be summarized that to avoid the formation of multiradicals, the mainly planar FPAH's with hexagonal rings undergo rearrangement to include both hexagonal and pentagonal rings, which results in the closed curved 3-D structures typical of fullerenes.

ACKNOWLEDGMENTS

We thank the Post Graduated Cooperation Program between France and Venezuela for the partial financial support of this work. Additionally, the financial support from the Conseil Régional d'Aquitaine (20071303002PFM) and FEDER (31486/08011464) is acknowledged.

NOMENCLATURES

CDA	: Coal derived asphaltenes
CR	: Cation radical
CN	: Cerro Negro
FPAHs	: Fused polycyclic aromatic hydrocarbons
IPR	: Isolated pentane rule
LS	: Laser shots
LDI-TOF	: Laser desorption/ionization-time of flight
MM	: Molecular mass
MMD	: Molecular mass distribution
MS	: Mass spectrometry
PAHs	: Polycyclic aromatic hydrocarbons
RTEM	: Resolution transmission electron microscopy
TWIM	: Traveling wave ion mobility

REFERENCES

1. Pereira T. M. C., Vanini G., Tose L.V., Cardoso F. M. R., and et al., "FT-ICR MS Analysis of Asphaltenes: Asphaltenes Go in, Fullerenes Come Out," *Journal of Fuel*, **2014**, *131*, 49-58.
2. Rizzi A., Cosmina P. Flego C., Montanari L., Seraglia R., and et al., "Laser Desorption/ Ionization Techniques in the Characterization of High Molecular Weight Oil Fractions. Part 1: Asphaltenes," *Journal of Mass Spectrometry*, **2006**, *41*, 1232-1241.
3. Palacio L., Orrego-Ruiz J. A., Barrow M. P., Hernandez R. C., and et al., "Analysis of the Molecular Weight Distribution of Vacuum Residues and their Molecular Distillation Fractions by Laser Desorption Ionization Mass Spectrometry," *Journal of Fuel*, **2016**, *171*, 247-252.
4. Hortal A. R., Hurtado P., Martínez-Haya B., and Mullins O. C., "Molecular-weight Distributions of Coal and Petroleum Asphaltenes from Laser Desorption/ionization Experiments," *Journal of Energy and Fuels*, *21*, 2863-2868.
5. Apicella B., Alfè M., Amoresano A., Galano E., and Ciajolo A., "Advantages and Limitations of Laser Desorption/ionization Mass Spectrometric Techniques in the Chemical Characterization of Complex Carbonaceous Materials," *International Journal of Mass Spectrometry*, **2010**, *295*, 98-102.
6. Gámez F., Hortal A. R., Martínez-Haya B., Soltwisch J., and et al., "Ultraviolet Laser

Desorption/ionization Mass Spectrometry of Single-core and Multi-core Polyaromatic Hydrocarbons under Variable Conditions of Collisional Cooling: Insights into the Generation of Molecular Ions, Fragments and Oligomers," *Journal of Mass Spectrometry*, **2014**, *49*, 1127-1138.

7. Daaou M., Modarressi A., Bendedouch D., Bouhadda Y., Krier G., and et al., "Characterization of the Nonstable Fraction of Hassi–Messaoud Asphaltenes," *Journal of Energy and Fuels*, **2008**, *22*, 3134-3142.
8. Santos V. G., Fasciotti M., Pudenzi M. A., Klitzke C. F., and et al., "Fullerenes in Asphaltenes and other Carbonaceous Materials: Natural Constituents or Laser Artifacts," *Journal of Analyst*, **2016**, *141*, 2767-2773.
9. Buseck P. R., Tsipursky S. J., and Hettich R., "Fullerenes from the Geological Environment," *Journal of Science*, **1992**, *257*, 215-217.
10. Becker L., Bada J. L., Winans R. E., Hunt J. E., and et al., "Fullerenes in the 1.85-billion-year-old Sudbury Impact Structure," *Journal of Science*, **1994**, *265*, 642-645.
11. Daaou M., Larbi A., Martínez-Haya B., and Rogalski M., "A Comparative Study of the Chemical Structure of Asphaltenes from Algerian Petroleum Collected at Different Stages of Extraction and Processing," *Journal of Petroleum Science and Engineering*, **2016**, *138*, 50–56.
12. Fergoug T., Boukratem C., Bounaceur B, and Bouhadda Y., "Laser Desorption/Ionization-Time of Flight (LDI-TOF) and Matrix-Assisted Laser Desorption/Ionization-Time of Flight (MALDI – TOF) Mass Spectrometry of an Algerian Asphaltene," *Egyptian Journal of Petroleum*, **2016**, *26*(3), 803-810.
13. Becker C., Qian K., and Russell D. H., "Molecular Weight Distributions of Asphaltenes and Deasphaltened Oils Studied by Laser Desorption Ionization and Ion Mobility Mass Spectrometry," *Journal of Analytical Chemistry*, **2008**, *80*, 8592–8597.
14. Camacho-Bragado G. A., Espinosa M. M., Romero E. T., Murgich J., and et al., "Fullerenic Structures derived from Oil Asphaltenes," *Journal of Carbon*, **2002**, *40*, 2761–2766.
15. Koolen H. H. F., Klitzke C. F., Cardoso F. M. R., Rosa P. T. V., and et al., "Fullerene Separation and Identification by Traveling Wave ion Mobility Mass Spectrometry in Laser Desorption Processes during Asphaltene Analysis," *Journal of Mass Spectrom*, **2005**, *51*, 254–256.
16. Zhen J., Castellanos P., Paardekooper D., Linnartz H., and et al., "Laboratory Formation of Fullerenes from PAHs: Top-Down Interstellar Chemistry," *The Astrophysical J. Letters*, **2014**, *797*, 30.
17. Acevedo S., Escobar G., Ranaudo M. A., and Rizzo A., "Molecular Weight Properties of Asphaltenes Calculated from GPC Data for Octylated Asphaltenes," *Journal of Fuel*, **1998**, *77*(8), 853-858.
18. Wu Q., Pomerantz, A. E. Mullins O. C., and Zare R. N., "Laser-based Mass Spectrometric Determination of Aggregation Numbers for Petroleum and Coal-derived Asphaltenes," *Journal of Energy and Fuels*, **2014**, *28*, 475-482.
19. Mahajan T. B., Elsila J. E., Deamer D. W., and Zare R. N., "Formation of Carbon-carbon Bonds in the Photochemical Alkylation of Polycyclic

Aromatic Hydrocarbons," *Journal of Origins of Life & Evolution of the Biosphere*, **2003**, *33*, 17-35.

20. Lobato M. D., Pedrosa J. M., Hortal A. R., Martínez-Haya B., and et al., "Characterization and Langmuir Film Properties of Asphaltenes Extracted from Arabian Light Crude Oil," *Colloids and Surfaces A: Physicochemical and Engineering Aspects*, **2007**, *298*, 72–79.
21. Araujo P., Mendes M., and Oller N., "Contribution of Mass Spectrometry for Assessing Quality of Petroleum Fractions," *Journal of Petroleum Science & Engineering,* **2013**, *109*, 198-205.
22. Pope C. and Howard J., "Thermochemical Properties of Curved PAH and Fullerenes- a Group Additivity Method Compared with mm^3(92) and Mopac Predictions," *Journal of Physical Chemistry*," **1995**, *99*, 4306-4316.
23. Pope C. J., Marr J. A., and Howard J. B., "Chemistry of Fullerenes C_{60} and C_{70} Formation in Flames," *Journal of Physical Chemistry*, **1993**, *97*, 11001-11013.
24. Acevedo S., Mendez B., Rojas A., Layrisse I., and et al., "Asphaltenes and Resins from the Orinoco Basin," *Journal of Fuel*, **1985**, *64*, 1741-1747.
25. Stewart J. J. P., "Optimization of Parameters for Semi-empirical Methods V: Modification of NDDO Approximations and Application to 70 Elements," *Journal of Molecular Modeling*, **2007**, *13*, 1173-1213.
26. Brinkmann G., Goedgebeur J., and McKay B. D., "The Generation of Fullerenes," *Journal of Chemical Information and Modeling*, **2012**, *52*, 2910-2918.
27. Acevedo S., Gutiérrez L., Negrin G., Pereira J., and et al., "Molecular Weight of Petroleum Asphaltenes: A Comparison between Mass Spectrometry and Vapor Pressure Osmometry," *Journal of Energy & Fuels*, **2005**, *19,* 1548-1560.
28. Yen, T. F., "Structural Differences between Asphaltenes Isolated from Petroleum and from Coal Liquid," *Journal of Chemistry of Asphaltenes*, **1981**, *195*, 39-51.
29. Phipps C., "Laser Ablation and its Applications Laser Ablation of Energetic Polymer Solutions: Effect of Viscosity and Fluence on the Splashing Behavior," *Journal of Applied Physics A, Springer*, **2009**, *94*(3), 657-665.
30. Cash G. G., "Heats of Formation of Curved PAH's and C_{60}: Graph Theoretical vs MM3(92) Predictions," *Journal of Physical Chemistry A,* **1997**, *101*, 8094-8097.
31. Yen T. F., "Structural Differences between Asphaltenes Isolated from Petroleum and from Coal Liquid," *Journal of Chemistry of Asphaltenes*, **1981**, *195*, 39-51.
32. Brinkmann G., Goedgebeur J., and McKay B. D., "The Generation of Fullerenes," *Journal of Chemical Information and Modeling*, **2012**, *52*, 2910-2918.